IOPscience iopscience.iop.org

Home Search Collections Journals About Contact us My IOPscience

Fast, multicolor photodetection with graphene-contacted p-GaSe/n-InSe van der Waals heterostructures

This content has been downloaded from IOPscience. Please scroll down to see the full text.

Download details:
This content was downloaded by: ppzap2
IP Address: 128.243.187.166
This content was downloaded on 23/05/2017 at 09:52

Manuscript version: Accepted Manuscript
Yan et al

To cite this article before publication: Yan et al, 2017, Nanotechnology, at press: https://doi.org/10.1088/1361-6528/aa749e

This Accepted Manuscript is: © 2017 IOP Publishing Ltd

During the embargo period (the 12 month period from the publication of the Version of Record of this article), the Accepted Manuscript is fully protected by copyright and cannot be reused or reposted elsewhere.

As the Version of Record of this article is going to be / has been published on a subscription basis, this Accepted Manuscript is available for reuse under a CC BY-NC-ND 3.0 licence after the 12 month embargo period.

After the embargo period, everyone is permitted to copy and redistribute this article for non-commercial purposes only, provided that they adhere to all the terms of the licence https://creativecommons.org/licences/by-nc-nd/3.0

Although reasonable endeavours have been taken to obtain all necessary permissions from third parties to include their copyrighted content within this article, their full citation and copyright line may not be present in this Accepted Manuscript version. Before using any content from this article, please refer to the Version of Record on IOPscience once published for full citation and copyright details, as permission will likely be required. All third party content is fully copyright protected, unless specifically stated otherwise in the figure caption in the Version of Record.

When available, you can view the Version of Record for this article at: http://iopscience.iop.org/article/10.1088/1361-6528/aa749e

Fast, multicolor photodetection with graphene-contacted p-GaSe/n-InSe van der Waals heterostructures

Faguang Yan[1], Lixia Zhao[2,3], Amalia Patanè[4], PingAn Hu[5], Xia Wei[1], Wengang Luo[1], Dong Zhang[1], Quanshan Lv[1], Qi Feng[1], Chao Shen[1,3], Kai Chang[1,3], Laurence Eaves[4] and Kaiyou Wang[1,3]

[1] State Key Laboratory of Superlattices and Microstructures, Institute of Semiconductors, Chinese Academy of Sciences, Beijing 100083, China

[2] State Key Laboratory of Solid-State Lighting, Institute of Semiconductors, Chinese Academy of Sciences, Beijing 10083, China

[3] College of Materials Science and Opto-Electronic Technology, University of Chinese Academy of Science, Beijing 100049, China

[4] School of Physics and Astronomy, University of Nottingham, Nottingham NG7 2RD, UK.

[5] Key Lab of Microsystem and Microstructure, Harbin Institute of Technology, Ministry of Education, Harbin, 150080, China

E-mail: kywang@semi.ac.cn

Keywords: Multicolor, gallium selenide, indium selenide, van der Waals heterostructure, built-in potential

Accepted Manuscript

Abstract

The integration of different two-dimensional materials within a multilayer van der Waals (vdW) heterostructure offers a promising technology for high performance opto-electronic devices such as photodetectors and light sources. Here we report on the fabrication and electronic properties of vdW heterojunction diodes composed of the direct band gap layered semiconductors InSe and GaSe and transparent monolayer graphene electrodes. We show that the type II band alignment between the two layered materials and their distinctive spectral response, combined with the short channel length and low electrical resistance of graphene electrodes, enable efficient generation and extraction of photoexcited carriers from the heterostructure even when no external voltage is applied. Our devices are fast (~ 1 μs), self-driven photodetectors with multicolor photoresponse ranging from the ultraviolet to the near-infrared and offer new routes to miniaturized optoelectronics beyond present semiconductor materials and technologies.

Introduction

Multicolor photodetectors covering the ultraviolet (UV), visible and infrared (IR) spectral ranges have potential for a wide range of applications, such as optical communication [1, 2], imaging [3], environmental monitoring [4] and astronomical observations [5]. Furthermore, robust and miniaturized self-driven devices, which require no electrical power source, are of particular interest for applications in extreme conditions. Self-driven multicolor photodetectors using semiconductor heterojunctions, such as MoS_2/Si [6], CuO/Si [7], Bi_2Se_3/Si [8] and MoS_2/GaAs heterojunctions [9], have attracted considerable attention recently. Photodetectors based on van der Waals (vdW) heterostructures have also been demonstrated [10, 11]. However, self-driven "multicolor" photodetectors that require no external power

Accepted Manuscript

1 2 3 4 5 6 7 8 9 10 11 12 13 14 15 16 17 18 19 20 21 22 23 24 25 26 27 28 29 30 31 32 33 34 35 36 37 38 39 40 41 42 43 44 45 46 47 48 49 50 51 52 53 54 55 56 57 58 59 60

source are more difficult to realize. VdW heterostructures, which can be assembled by stacking different two-dimensional (2D) semiconductors with different bandgaps, can combine and exploit the properties of the component materials within a single device. Such structures are therefore candidates for multifunctional optoelectronic systems with superior performance. In contrast to gapless graphene [12], GaSe [13] and InSe [14] and monolayers of the transition metal dichalcogenides (TMDCs) [15,16], are direct band gap semiconductors. High performance photodetectors based on few-layered *p*-type GaSe or *n*-type InSe have been reported previously [17-19]. In addition to their response to visible light, the photoresponse of 2D GaSe photodetectors [13] can extend into the ultraviolet (UV) region, while InSe nanosheets show strong near-infrared (NIR) photoluminescence (PL) emission and photoresponsivity [20]. These results suggest that a heterojunction based on 2D *p*-GaSe and *n*-InSe could be used for photodetection over a still broader spectral range.

Although vdW heterostructures with metal electrodes have been studied extensively and demonstrate interesting optoelectronic and electronic properties [21, 22], their response time ranges from milliseconds [23] to seconds [24]. To fabricate faster, higher-performance devices, it is essential that the optically active layers have good interfaces and Ohmic contacts. In contrast to metal-contacted photodetectors, the near perfect optical transparency and the unique electronic properties of graphene make it an ideal electrode for multilayer, “vertical” vdW heterostructures as it can act as a short, atomically thin charge extraction channel with a large active area, thus enabling both fast and efficient photodetection [19]. An effective method to create faster vdW heterostructure photodetectors is therefore to sandwich the heterojunction between two layers of graphene, which act as electrodes. These heterostructures can be fabricated with clean interfaces free from dangling bonds, with low defect density and without the

Accepted Manuscript

1
2
3
4
5
6
7
8
9
10
11
12
13
14
15
16
17
18
19
20
21
22
23
24
25
26
27
28
29
30
31
32
33
34
35
36
37
38
39
40
41
42
43
44
45
46
47
48
49
50
51
52
53
54
55
56
57
58
59
60

Fermi-level pinning that often occurs when metal contacts are directly deposited onto a semiconductor surface.

Here we report on graphene contacted *p*-GaSe/*n*-InSe heterojunctions. A typical device structure is shown schematically in figure 1(a). A GaSe layer is placed directly on top of the InSe sheet. This sequence of layers ensures that photons of energy $hv < 2$ eV are transmitted through the wide band gap energy GaSe ($E_g = 2.05$ eV at 300K) and can excite electron-hole pairs in the smaller band gap InSe ($E_g = 1.26$ eV at 300K). This large area (~ 50 μm^2) *p*-GaSe/*n*-InSe heterojunction exhibits a strong self-driven photoresponse ranging from the UV to NIR due to the built-in potential in the heterojunction, the type-II band alignment between the two layered crystals [25] and their distinctive band gap energies. Furthermore, using graphene rather than metals as electrodes enable a response time as short as 1.85 μs, *i.e.* significantly faster than that reported recently for van der Waals diode-like photodetectors [10, 22, 23], and 3 to 5 orders of magnitude faster than previously reported for photodetectors based on GaSe [13, 26, 27] or InSe alone [19, 28], which usually have a slow response due to the presence of carrier traps in the relatively long active region of the detector [1, 29, 30].

Results and discussion

Figure 1(b) shows high-resolution transmission electron microscopy images and electron diffraction patterns of the β-GaSe and β-InSe layers. These have high crystalline quality and in-plane hexagonal symmetry. Their crystal structure consists of Se-M-M-Se (M represents Ga- and In- atoms) layers, as shown in the Supplementary Information figure S1. The measured in-plane lattice constants of GaSe and InSe are $a = 0.37$ and 0.4 nm, respectively. The separations of two neighboring tetralayers of GaSe and

Accepted Manuscript

1
2
3
4
5
6
7
8
9
10
11
12
13
14
15
16
17
18
19
20
21
22
23
24
25
26
27
28
29
30
31
32
33
34
35
36
37
38
39
40
41
42
43
44
45
46
47
48
49
50
51
52
53
54
55
56
57
58
59
60

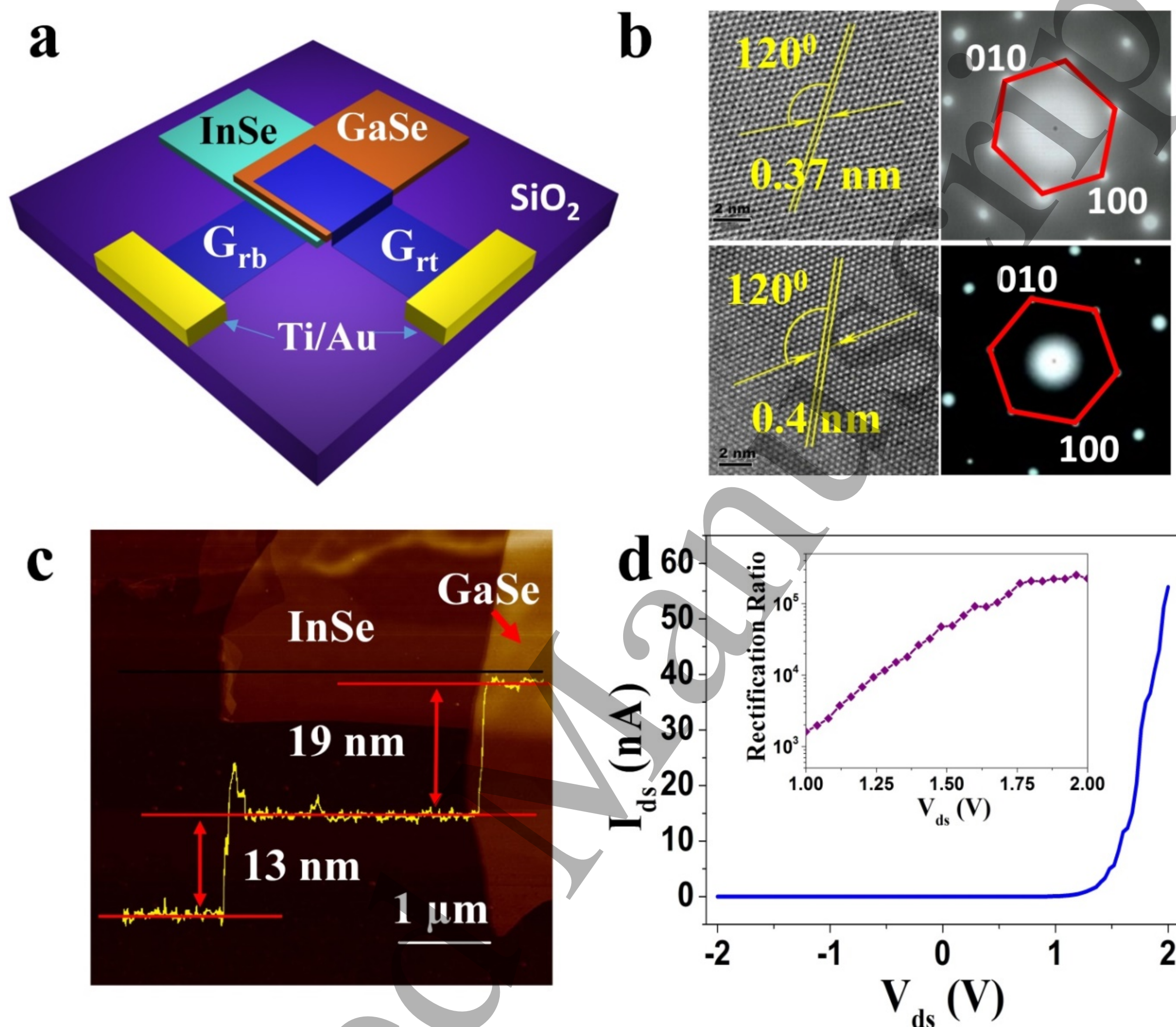

Figure 1. Schematic diagram and current-voltage *I*-*V* characteristic of the *p*-GaSe/*n*-InSe heterojunction diode. (a) Schematic diagram of the *p*-GaSe/*n*-InSe heterojunction diode. (b) High-resolution TEM image of the GaSe (top left) and InSe (bottom left), respectively. Images on the right show the corresponding electron-beam diffraction patterns of GaSe and InSe. (c) AFM image of the device. The inset shows the thickness of the different layers. (d) The *I*-*V* characteristic of the *p*-GaSe/*n*-InSe heterojunction diode at room temperature. The inset shows the rectification ratio as a function of the source-drain voltage V_{ds}.

InSe are d = 0.9 and 0.84 nm, respectively. For the fabrication of the heterostructure, graphene microstamps were first transferred onto a fused silica substrate to form one electrode. The InSe flake was

Accepted Manuscript

1
2
3
4
5
6
7
8
9
10
11
12
13
14
15
16
17
18
19
20
21
22
23
24
25
26
27
28
29
30
31
32
33
34
35
36
37
38
39
40
41
42
43
44
45
46
47
48
49
50
51
52
53
54
55
56
57
58
59
60

Accepted Manuscript

mechanically exfoliated using adhesive tape from bulk single crystals onto a stamp and then transferred onto the graphene electrode. Using the same method, the GaSe sheet was transferred on top of the InSe sheet. Finally, a second graphene microstamp was transferred onto the GaSe sheet to form the top electrode (see also the Supplementary Information). Room temperature measurements of the electrical properties of the heterojunction diode reveal strong rectification in the current-voltage (*I-V*) characteristics, with a larger current passing when the *p*-type GaSe is positively biased relative to *n*-type InSe (figure 1(d)). The rectification ratio, defined as the ratio of the forward/reverse current, reaches ~10^5 at V_{ds}= +2/-2 V (figure 1(d), inset), demonstrating that a good *p-n* diode is formed within the atomically thin GaSe/InSe heterojunction.

Figure 2 shows the dependence of the *I-V* characteristics on light intensity *P* ranging from 0 to 50 mW cm^{-2}. The source-drain current I_{ds} increases with increasing *P* (figure 2(a)) and the photocurrent I_{ph} exhibits sublinear behavior, *i.e.* $I_{ph} \propto P^{\alpha}$, where α = 0.84, 0.80 and 0.45 at source-drain voltages of V_{ds} = -2, 0 and 2 V, respectively (figure 2(b)). A similar sublinear response has also been reported for other nanomaterials, such as ZnO [31] and GaN nanowires [32], WSe_2/Graphene [30] and MoS_2/WS_2 heterostructures [33]. This response suggests a decrease of the recombination time of carriers with increasing *P* due Auger recombination processes. We also note that in forward bias, due to the high injection of majority carriers across the junction, Auger recombination could be enhanced thus leading to a different power dependence of the photocurrent.

Figures 2(c) and (d) plot the photoresponsivity ($R=I_{ph}/PS$) and detectivity ($D^*=RS^{1/2}/(2eI_{dark})^{1/2}$) of the heterojunction at different applied voltages as a function of incident light intensity. Here *S* is the in-plane area (50 μm^2) of the device, *e* is the electron charge and I_{dark} is the dark current. Both *R* and *D** increase

1
2
3
4
5
6
7
8
9
10
11
12
13
14
15
16
17
18
19
20
21
22
23
24
25
26
27
28
29
30
31
32
33
34
35
36
37
38
39
40
41
42
43
44
45
46
47
48
49
50
51
52
53
54
55
56
57
58
59
60

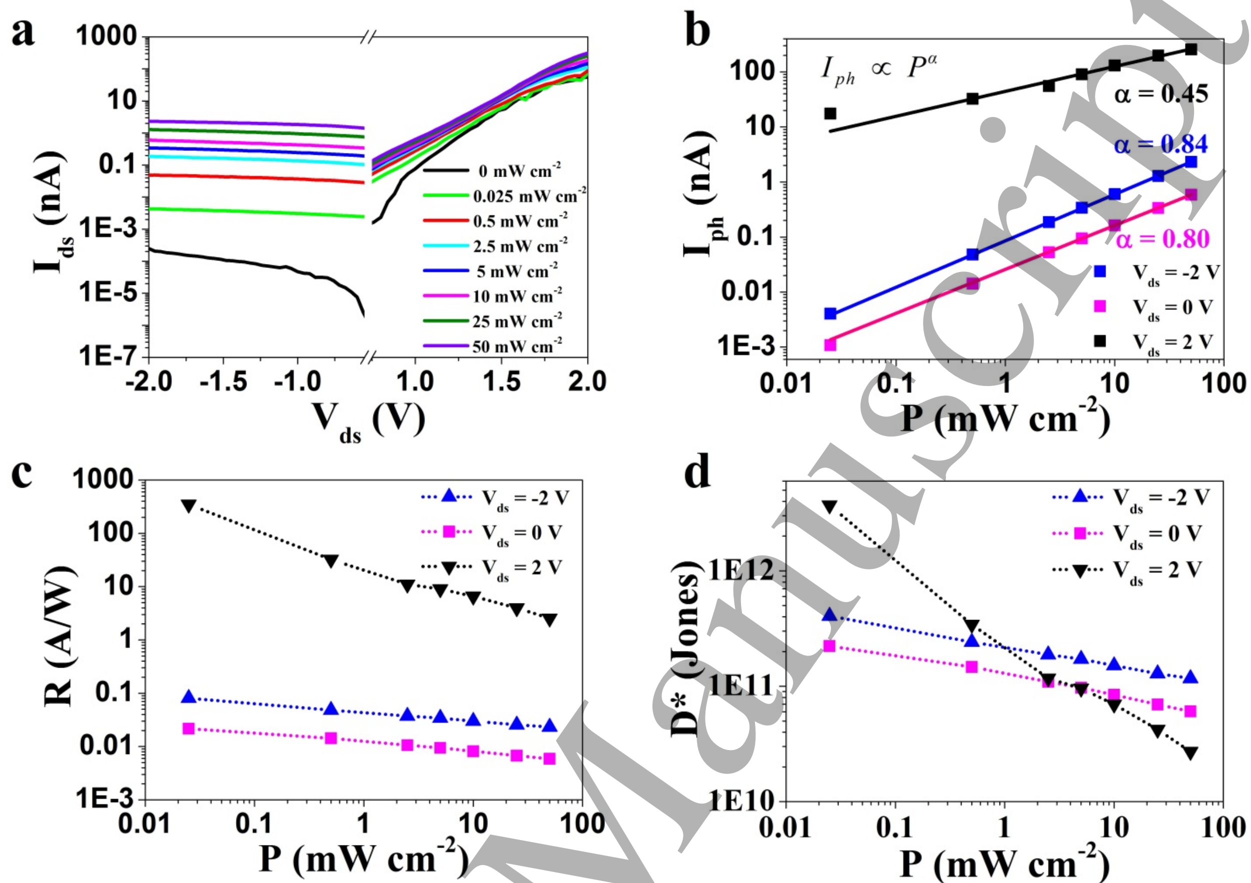

Figure 2. Power-dependent optoelectronic characterization at different applied voltages V_{ds}. (a) Typical I_{ds} curves of the *p*-GaSe/*n*-InSe heterojunction diode with illumination at various excitation intensities (P = 0, 0.025, 0.5, 2.5, 5, 10, 25, 50 mW cm^{-2}) and wavelength λ = 410 nm at room temperature. (b) Photocurrent as a function of the illumination intensity at different V_{ds} (forward bias V_{ds} = 2 V, zero bias V_{ds} = 0 V and reverse bias V_{ds} = -2 V). The solid lines are fits to the data. (c,d) Photoresponsivity R (c) and detectivity D^* (d) of the heterojunction diode as a function of the illumination intensity P at different V_{ds} (V_{ds} = 2, 0, -2 V). The spot size of the laser beam is about 0.2 mm^2, which is much larger than the device size.

with decreasing light intensity, consistent with the sublinear behavior of the photocurrent. The decrease of R with increasing P is common to many photodetectors. It suggests a decrease of the recombination time

Accepted Manuscript

1
2
3
4
5
6
7
8
9
10
11
12
13
14
15
16
17
18
19
20
21
22
23
24
25
26
27
28
29
30
31
32
33
34
35
36
37
38
39
40
41
42
43
44
45
46
47
48
49
50
51
52
53
54
55
56
57
58
59
60

of carriers with increasing P due Auger recombination processes; further, an increasing P can also increase the carrier transit time due to increased carrier scattering.

The response of a photodetector is determined by a combination of several processes, including the excitation, recombination, and diffusion of carriers. Due to the built-in potential of the heterojunction and the type II band alignment (figure 3(a)), at zero bias the photocreated electrons and holes are swept in opposite directions across the junction into the graphene electrodes (figure 3(b)). We estimate that the built-in potential of the heterostructure is about 0.6 V (see Supplementary Information, figure S2). Thus our devices can operate at zero bias with a photoresponsivity of up to $R = 21$ mA W^{-1} with corresponding detectivity $D^* = 2.2\times10^{12}$ Jones at $\lambda = 410$ nm. The systematic decrease of R and D^* with increasing P can arise from stronger Coulomb interactions between the photogenerated carriers and enhanced radiative/non-radiative recombination. A reverse bias voltage increases I_{ph} and R due to the increased electric field in the junction, which decreases the carrier transit time, resulting in reduced carrier recombination (figure 3(c)). We also note that I_{ph} and R are strongly enhanced in applied forward biases beyond the open circuit voltage V_{oc} (*e.g.* $I_{ds} = 0$) and at high V. In this regime, due to the high injection of majority carriers across the junction, the influence of carrier traps is weaker and a larger number of photogenerated carriers are effectively extracted across the thin layers into the graphene electrodes (figures 3(d) and (e)).

In our devices, a photoresponsivity of up to $R = 350$ A W^{-1} is obtained at $V_{ds} = 2$ V with an illumination intensity $P = 0.025$ mW cm^{-2} and $\lambda = 410$ nm. This value of R is 2 to 3 orders of magnitude larger than for heterojunction photodetectors based on transition-metal dichalcogenides (TMDCs) such as MoS_2/WSe_2 [21, 34] and $MoTe_2/MoS_2$ [23]. The corresponding detectivity is estimated to be $D^* = 3.7\times10^{12}$ Jones,

Accepted Manuscript

1
2
3
4
5
6
7
8
9
10
11
12
13
14
15
16
17
18
19
20
21
22
23
24
25
26
27
28
29
30
31
32
33
34
35
36
37
38
39
40
41
42
43
44
45
46
47
48
49
50
51
52
53
54
55
56
57
58
59
60

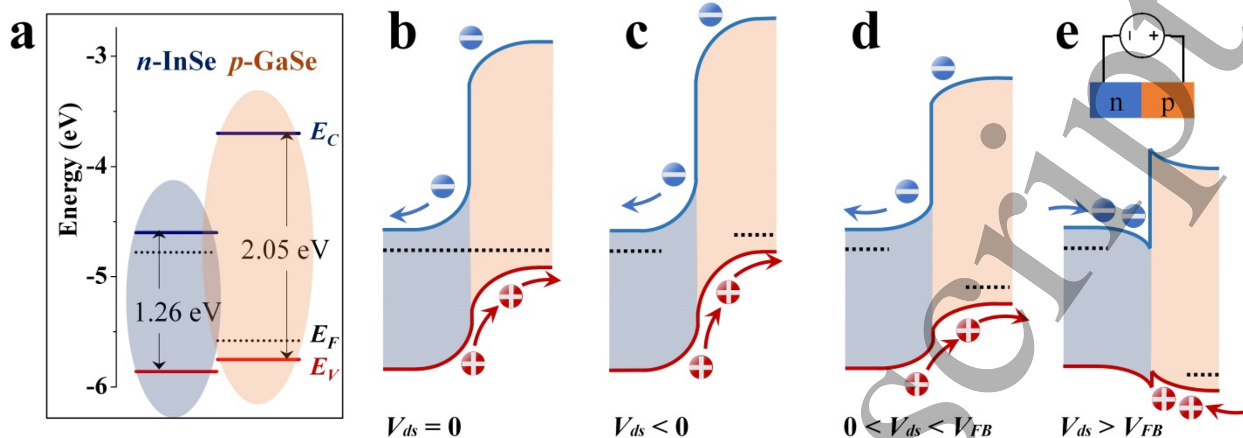

Figure 3. Band alignment at the interface of the *p*-GaSe/*n*-InSe heterojunction. (a) Band alignment for isolated *n*-InSe and *p*-GaSe layers. Electron affinities of InSe and GaSe are χ = -4.6 and -3.7 eV, respectively. The conduction minimum (CB) of GaSe lies above that of InSe by ΔE_c = 0.9 eV whereas the valence band (VB) edge of InSe lies below (ΔE_v = -0.1 eV) that of the larger band gap GaSe, resulting in a type II band alignment. (b,c,d,e) Schematic band alignment at the interface of the heterojunction at different applied voltages V_{ds} (reverse bias (c), zero bias (b) and forward bias (d,e)). V_{FB} is the voltage corresponding to the flat band condition.

which is two orders of magnitude higher than that of InGaAs/InGaP-based [35] and MoS_2-based [36] photodetectors, and is similar to that of Si *p*-*n* junction photodetectors [37]. These high *R* and *D** values indicate that the *p*-GaSe/*n*-InSe vertical heterojunction is extremely sensitive to small optical input signals. Furthermore, these devices can operate with no externally applied voltage, thus they have potential for applications that require miniaturized devices with minimal energy consumption.

The spectral response of the *p*-GaSe/*n*-InSe heterojunction in figure 4(a) demonstrates a strong photoresponsivity over the range λ = 270-920 nm, from UV to NIR, under both reverse and zero biases. The photoresponsivity in both reverse bias, V_{ds} = -2 V, and zero bias display a similar wavelength

Accepted Manuscript

1
2
3
4
5
6
7
8
9
10
11
12
13
14
15
16
17
18
19
20
21
22
23
24
25
26
27
28
29
30
31
32
33
34
35
36
37
38
39
40
41
42
43
44
45
46
47
48
49
50
51
52
53
54
55
56
57
58
59
60

dependence. The peak in the photoresponsivity between 400 and 500 nm corresponds to excitations between the p_{xy}-like orbitals at the top of the valence band of GaSe and the minimum of the conduction band of InSe. The UV response at λ = 270 and 350 nm is due to interband optical absorption in the GaSe layer, as for the case of GaSe-based photodetectors [13, 38]. The photoresponse in the NIR wavelength range arises from interband transitions in the InSe layer, which has a smaller band gap of 1.26 eV at room temperature [20]. To elucidate the role of graphene in our measurements, we have compared the photocurrent spectra of GaSe- and InSe-based photodetectors with metal and graphene electrodes, see new figure S3 in the supplementary information. A larger photoresponse was observed in photodetectors based on graphene electrodes. Based on the photocurrent and incident laser power, we can determine the external quantum efficiency, *EQE*, of the photon to electron conversion (figure 4(a)). The *EQE* ($= hcR/e\lambda$) is defined as the ratio of the number of carriers collected by the electrodes to the number of incident photons, and is wavelength dependent. At zero bias, the device has a maximum *EQE* of 9.3% at λ = 410 nm, higher than for monolayer MoS_2/Si *p-n* diodes [39].

To further explore the origin of the photoresponse, photocurrent maps were acquired at both zero and reverse biases. Figure 4(b) shows an optical microscope image of the Gr/GaSe/InSe/Gr heterostructure depicting the relative positions of the GaSe and InSe layers and of the graphene electrodes. The corresponding normalized photocurrent maps at zero and reverse biases with λ = 410 nm laser excitation (20 μW) are shown in figures 4(c) and (d), respectively. To distinguish the different parts of the heterostructure, the GaSe sheet region is outlined in green, the InSe sheet region in purple, and the top and bottom graphene electrodes in solid and dotted gold lines, respectively. The photocurrent map shows that the photosensitive region corresponds to the area where the four component layers

Accepted Manuscript

1 2 3 4 5 6 7 8 9 10 11 12 13 14 15 16 17 18 19 20 21 22 23 24 25 26 27 28 29 30 31 32 33 34 35 36 37 38 39 40 41 42 43 44 45 46 47 48 49 50 51 52 53 54 55 56 57 58 59 60

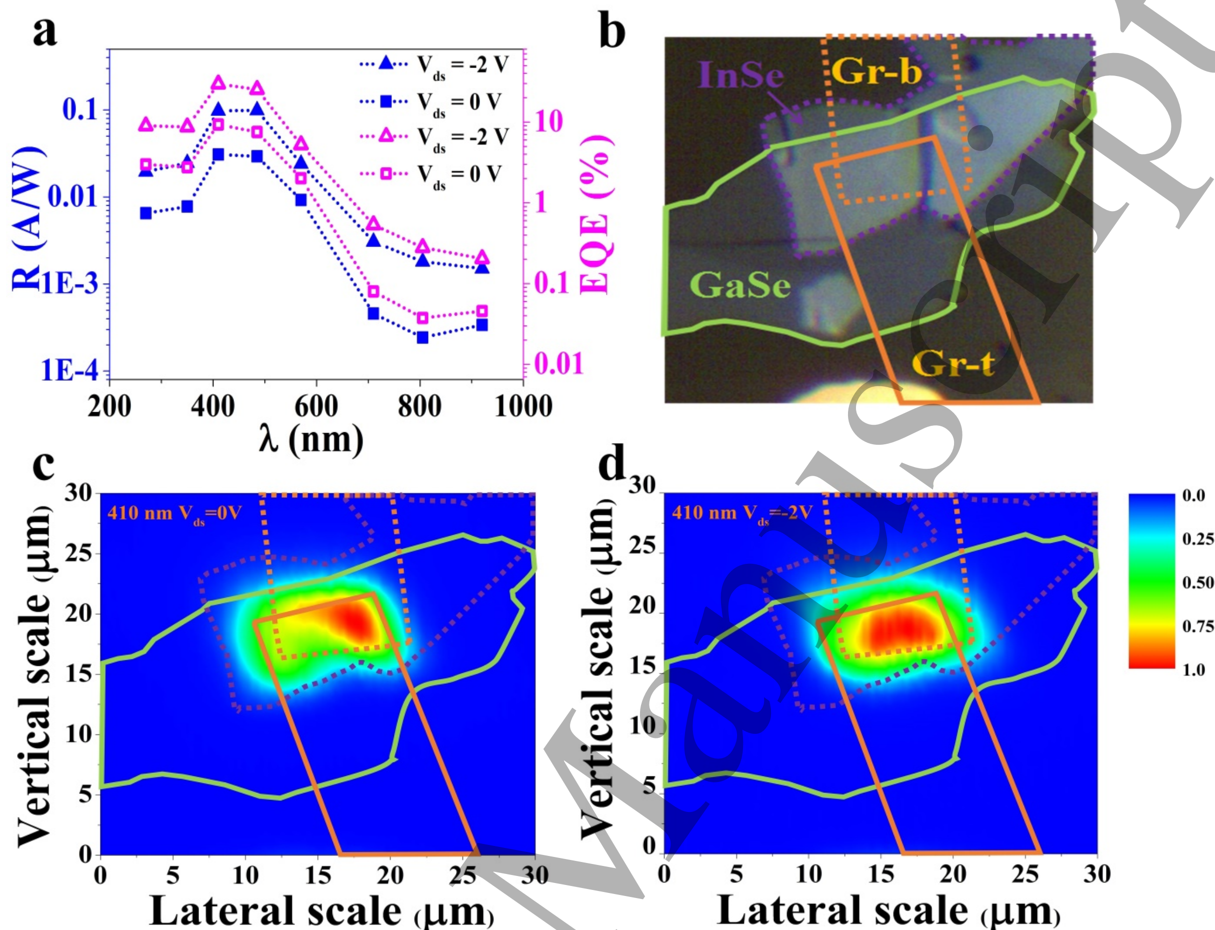

Figure 4. Spectral responsivity and normalized photocurrent maps of the *p*-GaSe/*n*-InSe heterojunction. (a) Room temperature photoresponsivity, *R*, and external quantum efficiency, *EQE*, as a function of illumination wavelength at different V_{ds} (V_{ds} = 0 V and V_{ds} = -2 V) and illumination intensity P = 1 mW cm^{-2}. The spot size of the laser beam is about 0.2 mm^2. (b) Optical microscope image of the heterojunction; t and b refer to top and bottom graphene electrodes. (c,d) Normalized photocurrent maps of the Gr/GaSe/InSe/Gr device obtained by scanning a focused laser beam at V_{ds} = 0 V (c) and -2 V (d) with wavelength λ = 410 nm (P = 20 μW). The green solid line outlines the GaSe sheet, the purple dotted line outlines the InSe sheet and the golden solid and dotted lines outline the top and bottom graphene electrodes, respectively. Photocurrent is observed where the 4 layers overlap. The laser beam is focused by a microscope objective onto a spot size of diameter of about 1.5 μm.

Accepted Manuscript

1
2
3
4
5
6
7
8
9
10
11
12
13
14
15
16
17
18
19
20
21
22
23
24
25
26
27
28
29
30
31
32
33
34
35
36
37
38
39
40
41
42
43
44
45
46
47
48
49
50
51
52
53
54
55
56
57
58
59
60

(Gr/GaSe/InSe/Gr) are superimposed and demonstrates the formation of a *p-n* junction across the area of the GaSe/InSe interface and the efficient extraction of carriers into the graphene electrodes. The weak photocurrent from the non-overlapping regions shows that the photogenerated carriers in the regions outside the *p-n* junction are separated and extracted less efficiently, even under a reverse bias V_{ds} = -2 V (figure 4(d)).

The response time is another important indicator of the performance of a photodetector. To assess their behavior in the time domain, the devices were illuminated with pulsed light generated by a light-emitting diode (LED) (λ = 470 nm) powered by a square-wave signal generator. As shown in figure 5(a), the dynamic response of the photocurrent at V_{ds} = 0 V is described well by the equations $I(t) = I_0\left[1 - \exp\left(-t/\tau_r\right)\right]$ and $I(t) = I_0\exp\left(-t/\tau_d\right)$, where τ_r = 5.97 μs and τ_d = 5.66 μs are the rise- and decay-time constants. The even faster photoresponse at V_{ds} = -2 V with τ_r = 1.85 μs and τ_d = 2.05 μs (figure 5(b)) is due to the enhanced electric field in reverse bias. Figures 5(c) and (d) show that the photocurrent can be switched on and off repeatedly and reproducibly with a square-wave modulation of the light intensity for different laser wavelengths (λ = 270, 350, 410, 485, and 570 nm) at a power P = 1 mW cm^{-2}. Similar switching behavior is observed for NIR photo-excitation (λ = 920 nm) under different illumination intensities for both zero and reverse biases (see Supplementary Information, figure S4). ON/OFF ratios up to 10^3 are observed, demonstrating that the heterojunction can be used as a sensitive and fast photo-detector. The measured response times are significantly faster than those recently reported for van der Waals heterojunction photodetectors [10, 19, 23, 24, 40] and Si-based heterojunction photodetectors [41, 42]. We also note that the measured response time is limited by the *RC*-time of our instrument and hence that a faster response could be obtained by improving the measuring circuit [43, 44].

Accepted Manuscript

1 2 3 4 5 6 7 8 9 10 11 12 13 14 15 16 17 18 19 20 21 22 23 24 25 26 27 28 29 30 31 32 33 34 35 36 37 38 39 40 41 42 43 44 45 46 47 48 49 50 51 52 53 54 55 56 57 58 59 60

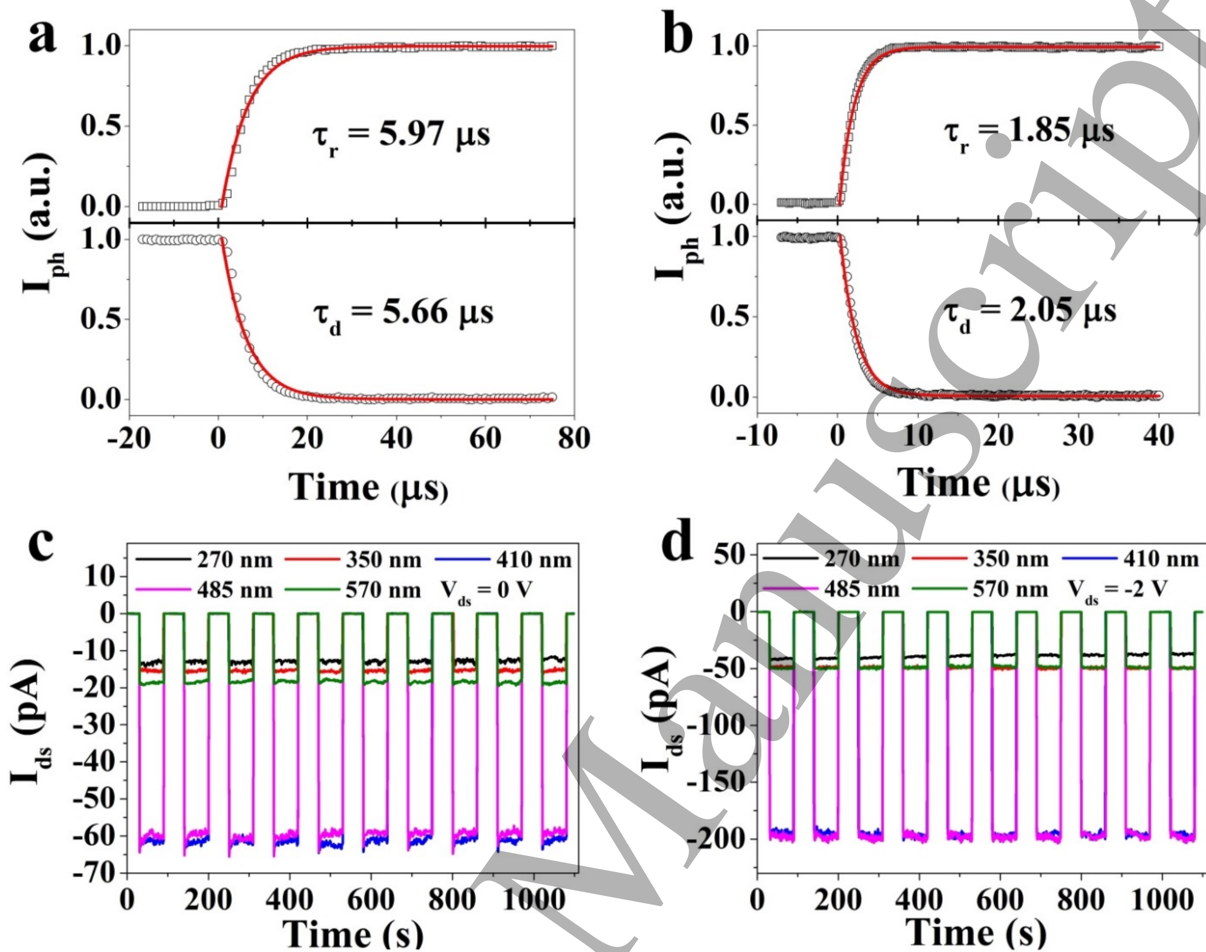

Figure 5. Response time and photo-switching of the *p*-GaSe/*n*-InSe heterojunction diode. (a,b) Temporal dependence of the photocurrent and times τ_r and τ_d at V_{ds} = 0 V (a) and V_{ds} = -2 V (b) at room temperature. The red solid lines are fits to the data. (c,d) Source-drain current I_{ds} as a function of time with photoswitching at V_{ds} = 0 V (c) and V_{ds} = -2 V (d) under illumination with different wavelengths (λ = 270, 350, 410, 485, and 570 nm) and light intensity P = 1 mW cm^{-2}. The spot size of the laser beam is about 0.2 mm^2.

Accepted Manuscript

1
2
3
4
5
6
7
8
9
10
11
12
13
14
15
16
17
18
19
20
21
22
23
24
25
26
27
28
29
30
31
32
33
34
35
36
37
38
39
40
41
42
43
44
45
46
47
48
49
50
51
52
53
54
55
56
57
58
59
60

Accepted Manuscript

Conclusion

In conclusion, we have reported on a novel van der Waals multi-layer heterostructure that combines several two-dimensional van der Waals crystals, *i.e.* graphene and the metal monochalcogenide InSe and GaSe layered semiconductors. The latter present a number of features that distinguish them from the widely explored TMDCs. In particular, they have a type II band alignment and have distinctive spectral response. We have exploited these features and the low electrical resistance and optical transparency of monolayer graphene electrodes to fabricate a junction diode that can adsorb light over a broad spectral range, from the ultraviolet, visible and infrared, and in which the photo-generated carriers can be efficiently and quickly extracted from the InSe/GaSe heterostructure even when no external voltage is applied. The low or zero energy consumption, simple heterostructure design and fast response time down to ~ 1 μs are notable important features of these nanometer-scale devices. Our results will stimulate further research into the science and technology of these heterostructures, which have the potential for a wide range of applications.

Acknowledgments

This work was supported by '973 Program' No. 2014CB643903, by the NSFC Grant No. 61225021, 11474272, 11174272, and 11404324, by the EU Graphene Flagship Project, and the Engineering and Physical Sciences Research Council (Grant No. EP/M012700/1). The Project was also sponsored by K. C. Wong Education Foundation.

References

[1] Konstantatos G and Sargent E H 2010 Nanostructured materials for photon detection *Nat. Nanotechnol.* **5**

391-400

[2] Huang Y, Duan X and Lieber C M 2005 Nanowires for integrated multicolor nanophotonics *Small* **1** 142-7

[3] Schermelleh L *et al* 2008 Subdiffraction multicolor imaging of the nuclear periphery with 3D structured illumination microscopy *Science* **320** 1332-6

[4] Formisano V, Atreya S, Encrenaz T, Ignatiev N and Giuranna M 2004 Detection of methane in the atmosphere of Mars *Science* **306** 1758-61

[5] Fontana A *et al* 2004 The K20 survey *Astron. Astrophys.* **424** 23-42

[6] Wang L, Jie J, Shao Z, Zhang Q, Zhang X, Wang Y, Sun Z and Lee S T 2015 MoS_2/Si heterojunction with vertically standing layered structure for ultrafast, high-detectivity, self-driven visible–near infrared photodetectors *Adv. Funct. Mater.* **25** 2910–9

[7] Hong Q, Cao Y, Xu J, Lu H, He J and Sun J-L 2014 Self-powered ultrafast broadband photodetector based on p–n heterojunctions of CuO/Si nanowire array *ACS Appl. Mater. Inter.* **6** 20887-94

[8] Zhang H, Zhang X, Liu C, Lee S-T and Jie J 2016 High-responsivity, high-detectivity, ultrafast topological insulator Bi_2Se_3/Silicon heterostructure broadband photodetectors *ACS Nano* **10** 5113-22

[9] Xu Z, Lin S, Li X, Zhang S, Wu Z, Xu W, Lu Y and Xu S 2016 Monolayer MoS_2/GaAs heterostructure self-driven photodetector with extremely high detectivity *Nano Energy* **23** 89-96

[10] Yang S *et al* 2016 Self-driven photodetector and ambipolar transistor in atomically thin GaTe-MoS_2 p–n vdW heterostructure *ACS Appl. Mater. Inter.* **8** 2533-9

[11] Huo N, Yang J, Huang L, Wei Z, Li S-S, Wei S-H and Li J 2015 Tunable polarity behavior and self-driven photoswitching in p-WSe_2/n-WS_2 heterojunctions *Small* **11** 5430-8

[12] Novoselov K S, Geim A K, Morozov S V, Jiang D, Zhang Y, Dubonos S V, Grigorieva I V and Firsov A A 2004

Accepted Manuscript

Electric field effect in atomically thin carbon films *Science* **306** 666

[13] Hu P, Wen Z, Wang L, Tan P and Xiao K 2012 Synthesis of few-layer GaSe nanosheets for high performance photodetectors *ACS Nano* **6** 5988-94

[14] Mudd G W, Svatek S A, Ren T, Patanè A, Makarovsky O, Eaves L, Beton P H, Kovalyuk Z D, Lashkarev G V and Kudrynskyi Z R 2013 Tuning the bandgap of exfoliated InSe nanosheets by quantum confinement *Adv. Mater.* **25** 5714-8

[15] Mak K F, Lee C, Hone J, Shan J and Heinz T F 2010 Atomically thin MoS_2: a new direct-gap semiconductor *Phy. Rev. Lett.* **105** 136805

[16] Zhao W, Ghorannevis Z, Chu L, Toh M, Kloc C, Tan P-H and Eda G 2013 Evolution of electronic structure in atomically thin sheets of WS_2 and WSe_2 *ACS Nano* **7** 791-7

[17] Cao Y, Cai K, Hu P, Zhao L, Yan T, Luo W, Zhang X, Wu X, Wang K and Zheng H 2015 Strong enhancement of photoresponsivity with shrinking the electrodes spacing in few layer GaSe photodetectors *Sci. Rep.* **5** 8130

[18] Luo W, Cao Y, Hu P, Cai K, Feng Q, Yan F, Yan T, Zhang X and Wang K 2015 Gate tuning of high-performance InSe-based photodetectors using graphene electrodes *Adv. Opt. Mater.* **3** 1418-23

[19] Mudd G W, Svatek S A, Hague L, Makarovsky O, Kudrynskyi Z R, Mellor C J, Beton P H, Eaves L, Novoselov K S and Kovalyuk Z D 2015 High broad‐band photoresponsivity of mechanically formed InSe‐graphene van der Waals heterostructures *Adv. Mater.* **27** 3760-6

[20] Mudd G W, Patanè A, Kudrynskyi Z R, Fay M W, Makarovsky O, Eaves L, Kovalyuk Z D, Zólyomi V and Falko V 2014 Quantum confined acceptors and donors in InSe nanosheets *Appl. Phys. Lett.* **105** 221909

[21] Lee C-H *et al* 2014 Atomically thin p–n junctions with van der Waals heterointerfaces *Nat. Nanotechnol.* **9** 676-81

Accepted Manuscript

1
2
3
4
5
6
7
8
9
10
11
12
13
14
15
16
17
18
19
20
21
22
23
24
25
26
27
28
29
30
31
32
33
34
35
36
37
38
39
40
41
42
43
44
45
46
47
48
49
50
51
52
53
54
55
56
57
58
59
60

[22] Cheng R, Li D, Zhou H, Wang C, Yin A, Jiang S, Liu Y, Chen Y, Huang Y and Duan X 2014 Electroluminescence and photocurrent generation from atomically sharp WSe_2/MoS_2 heterojunction p–n diodes *Nano Lett.* **14** 5590-7

[23] Pezeshki A, Shokouh S H H, Nazari T, Oh K and Im S 2016 Electric and photovoltaic behavior of a few‐layer α‐$MoTe_2/MoS_2$ dichalcogenide heterojunction *Adv. Mater.* **28** 3216-22

[24] Roy K, Padmanabhan M, Goswami S, Sai T P, Ramalingam G, Raghavan S and Ghosh A 2013 Graphene-MoS_2 hybrid structures for multifunctional photoresponsive memory devices *Nat. Nanotechnol.* **8** 826-30

[25] Balakrishnan N, Kudrynskyi Z R, Fay M W, Mudd G W, Svatek S A, Makarovsky O, Kovalyuk Z D, Eaves L, Beton P H and Patanè A 2014 Room temperature electroluminescence from mechanically formed van der Waals III–VI homojunctions and heterojunctions *Adv. Opt. Mater.* **2** 1064-9

[26] Yang S, Yue Q, Cai H, Wu K, Jiang C and Tongay S 2016 Highly efficient gas molecule-tunable few-layer GaSe phototransistors *J. Mater. Chem. C* **4** 248-53

[27] Zhou Y, Nie Y, Liu Y, Yan K, Hong J, Jin C, Zhou Y, Yin J, Liu Z and Peng H 2014 Epitaxy and photoresponse of two-dimensional GaSe crystals on flexible transparent mica sheets *ACS Nano* **8** 1485-90

[28] Tamalampudi S R, Lu Y-Y, Kumar U R, Sankar R, Liao C-D, Moorthy B K, Cheng C-H, Chou F C and Chen Y-T 2014 High performance and bendable few-layered InSe photodetectors with broad spectral response *Nano Lett.* **14** 2800-6

[29] Liu Y, Weiss N O, Duan X, Cheng H-C, Huang Y and Duan X 2016 Van der Waals heterostructures and devices *Nat. Rev. Mater.* **1** 16042

[30] Massicotte M, Schmidt P, Vialla F, Schädler K G, Reserbat Plantey A, WatanabeK, TaniguchiT, Tielrooij K J and Koppens F H L 2016 Picosecond photoresponse in van der Waals heterostructures *Nat. Nanotechnol.* **11** 42-6

Accepted Manuscript

[31] Soci C, Zhang A, Xiang B, Dayeh S A, Aplin D P R, Park J, Bao X Y, Lo Y H and Wang D 2007 ZnO nanowire UV photodetectors with high internal gain *Nano Lett.* **7** 1003-9

[32] González-Posada F, Songmuang R, Den Hertog M and Monroy E 2012 Room-temperature photodetection dynamics of single GaN nanowires *Nano Lett.* **12** 172-6

[33] Xue Y *et al* 2016 Scalable production of a few-layer MoS_2/WS_2 vertical heterojunction array and its application for photodetectors *ACS Nano* **10** 573-80

[34] Furchi M M, Pospischil A, Libisch F, Burgdörfer J and Mueller T 2014 Photovoltaic effect in an electrically tunable van der Waals heterojunction *Nano Lett.* **14** 4785-91

[35] Jiang J, Tsao S, O'Sullivan T, Zhang W, Lim H, Sills T, Mi K, Razeghi M, Brown G J and Tidrow M Z 2004 High detectivity InGaAs/InGaP quantum-dot infrared photodetectors grown by low pressure metalorganic chemical vapor deposition *Appl. Phys. Lett.* **84** 2166-8

[36] Tsai D-S, Liu K-K, Lien D-H, Tsai M-L, Kang C-F, Lin C-A, Li L-J and He J-H 2013 Few-layer MoS_2 with high broadband photogain and fast optical switching for use in harsh environments *ACS Nano* **7** 3905-11

[37] Gong X, Tong M, Xia Y, Cai W, Moon J S, Cao Y, Yu G, Shieh C-L, Nilsson B and Heeger A J 2009 High-detectivity polymer photodetectors with spectral response from 300 nm to 1450 nm *Science* **325** 1665

[38] Lei S, Ge L, Liu Z, Najmaei S, Shi G, You G, Lou J, Vajtai R and Ajayan P M 2013 Synthesis and photoresponse of large GaSe atomic layers *Nano Lett.* **13** 2777-81

[39] Lopez-Sanchez O, Alarcon Llado E, Koman V, Fontcuberta i Morral A, Radenovic A and Kis A 2014 Light generation and harvesting in a van der Waals heterostructure *ACS Nano* **8** 3042-8

[40] Ye L, Li H, Chen Z and Xu J 2016 Near-infrared photodetector based on MoS_2/black phosphorus heterojunction *ACS Photonics* **3** 692-9

Accepted Manuscript

[41] Lan C, Li C, Wang S, He T, Jiao T, Wei D, Jing W, Li L and Liu Y 2016 Zener tunneling and photoresponse of a WS_2/Si van der Waals heterojunction *ACS Appl. Mater. Inter.* **8** 18375-82

[42] Yan Z, Yu Y, Mi L, Hui W, Zhu Z, Wu Q, Zhang Y and Yang J 2016 In situ fabrication of vertical multilayered MoS_2/Si homotype heterojunction for high-speed visible–near-infrared photodetectors *Small* **12** 1062-71

[43] Zhang Y, Yu Y, Wang X, Tong G, Mi L, Zhu Z, Geng X and Jiang Y 2017 Solution assembly MoS_2 nanopetals/GaAs n-n homotype heterojunction with ultrafast and low noise photoresponse using graphene as carrier collector *Journal of Materials Chemistry C* **5** 140-8

[44] Longfei M, Hui W, Yan Z, Xudong Y, Yajing C, Guopeng L, Guohua L and Yang J 2017 High performance visible–near-infrared PbS-quantum-dots/indium Schottky diodes for photodetectors *Nanotechnology* **28** 055202

Accepted Manuscript